



Lateral distribution of N3 dye molecules on TiO₂(1 1 0) surface

Masatoshi Ikeda^a, Naoki Koide^b, Liyuan Han^{b,1}, Chi Lun Pang^c, Akira Sasahara^{a,d,*}, Hiroshi Onishi^a

^a Department of Chemistry, Faculty of Science, Kobe University, Nada-ku, Kobe 657-8501, Japan

^b Sharp Corporation, Hajikami, Katsuragi, Nara 639-2198, Japan

^c London Centre for Nanotechnology and Department of Chemistry, University College London, 20 Gordon Street, London WC1H 0AJ, United Kingdom

^d Japan Science and Technology Agency, Kawaguchi, Saitama 332-0012, Japan

ARTICLE INFO

Article history:

Received 7 August 2008

Received in revised form 27 October 2008

Accepted 1 December 2008

Available online 11 December 2008

Keywords:

N3

Titanium dioxide

Scanning tunneling microscopy

Aggregation

Autocorrelation analysis

ABSTRACT

The lateral distribution of Ru(4,4'-dicarboxy-2,2'-bipyridine)₂(NCS)₂ (N3) dye molecules on a titanium dioxide (TiO₂) surface was examined by using a scanning tunneling microscope. Pivalate ((CH₃)₃CCOO⁻)-covered rutile TiO₂(1 1 0) surfaces were immersed in acetonitrile containing the N3 dye. The N3 molecules which replaced the pivalates were observed as protrusions embedded in the pivalate monolayer. A two-dimensional radial distribution function indicated that the adsorbed N3 molecules tended to be aggregated. Trapping of an N3 molecule in the solution by a preadsorbed N3 molecule was proposed as a driving force for the aggregation. The hydrogen bonds between the carboxyl groups of two N3 molecules contribute to the trapping.

© 2008 Elsevier B.V. All rights reserved.

1. Introduction

Solar cells employing titanium dioxide (TiO₂) sensitized by dye molecules as an anode, known as dye-sensitized solar cells, have been under intensive study as promising substitutes for existing silicon-based solar cells, due to their low environmental loading, low product cost, and potentially high solar-to-electrical energy conversion efficiency [1,2]. The dye molecules which are adsorbed on the TiO₂ surface are excited by visible light and inject the photo-excited electrons into the conduction band of the TiO₂. The overall energy conversion efficiency has reached 11% under air mass 1.5 conditions [3], and further improvement of the efficiency is being attempted for practical use.

We have performed scanning probe microscope studies of dye-adsorbed rutile TiO₂(1 1 0) single crystal surfaces to collect information about nanoscale morphological and electronic structures of the dye-sensitized TiO₂ electrode surface [4–6]. The electron transfer through overlapping orbitals at the dye–TiO₂ interface should be sensitive to the nanoscale surface structures. As such, nanoscale analysis of the dye-adsorbed TiO₂ surface

may provide clues leading to the improvement of the electrode performance. Preferential adsorption of Ru(4,4'-dicarboxy-2,2'-bipyridine)₂(NCS)₂ (N3) dye at the step edges [6] and dependence of the Ru(4,4',4''-tricarboxy-2,2':6',2''-terpyridine)(NCS)₃ ("black dye") aggregation on the concentration of the deoxycholic acid additive in the dye solution [4] were shown with scanning tunneling microscope (STM) measurements. Kelvin probe force microscope analysis revealed a light-induced perturbation of work function on the N3 molecules, which indicated the possibility of monitoring electron transfer for individual dye molecules [5].

The present work focused on the lateral distribution of the N3 dye molecules on the TiO₂(1 1 0) surface as an extension to our previous STM studies. The two-dimensional radial distribution function of the N3 molecules was determined by applying an autocorrelation analysis to STM images. The lateral distribution of adsorbates often reflects the dynamics of the adsorption process [7–10] and therefore a detailed description of the aggregation process of the N3 molecules may be provided by the lateral distribution analysis. The aggregation is an important feature of the dye molecules related to the photoelectrochemical properties of the dye-sensitized electrode. It has been thought that the dye aggregation reduces the electron injection efficiency of the dye molecules due to intermolecular quenching of the excited states and the shading of the dye molecules anchored to the TiO₂ surface from the light [11–16]. On the other hand, enhanced energy conversion efficiency by a network of aggregated dye molecules has also been proposed, where an efficient reduction of the excited dye molecules by iodide ions in the electrolyte proceeds by hole transfer towards the dye molecules open to the electrolyte [17]. Clarifying the aggregation mechanism

* Corresponding author. Present address: School of Materials Science, Japan Advanced Institute of Science and Technology, 1-1 Asahidai, Nomi 923-1292, Japan. Tel.: +81 761 511503; fax: +81 761 511149.

E-mail address: sasahara@jaist.ac.jp (A. Sasahara).

¹ Present address: International Center for Materials Nano-Architectonics (MANA), National Institute for Materials Science (NIMS), 1-2-1 Sengen, Tsukuba, 305-0047 Japan.

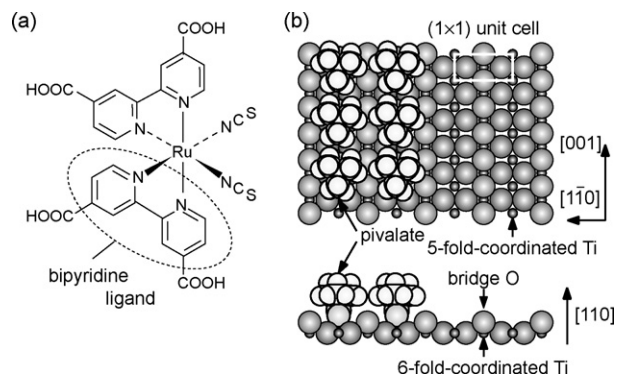


Fig. 1. Models of the (a) N3 molecule and (b) $\text{TiO}_2(1\ 1\ 0)-(1 \times 1)$ surface. The left half of the (1×1) surface is covered by pivalates.

provides a scheme for the control of the distribution of the dye molecules and thereby optimization of the electrode performance.

Fig. 1(a) shows the structure of the N3 molecule. Two bipyridine ligands and two thiocyanate (SCN) ligands are coordinated to a Ru(II) center with a C_2 symmetry around a bisection of the $\angle\text{NRuN}$ angle formed by the N atoms of the NCS groups [18,19]. The carboxyl groups (COOH) attached to the bipyridine ligands are bound to the surface Ti atoms of the TiO_2 [20–23]. Fig. 1(b) shows a ball model of the rutile $\text{TiO}_2(1\ 1\ 0)-(1 \times 1)$ surface [24]. The topmost O atoms are bound to two 6-fold-coordinated Ti atoms in a bridge coordination and form rows along the $[0\ 0\ 1]$ direction. Between the bridge O atom rows, Ti atoms coordinated to five O atoms (5-fold-coordinated Ti atoms) are exposed. The size of the unit cell is $0.30\ \text{nm} \times 0.65\ \text{nm}$.

2. Experimental

All experiments were performed with an ultra-high vacuum STM (JSPM4500S, JEOL) with a base pressure of 2×10^{-8} Pa. The microscope system was equipped with an ion sputtering gun (EX03, Thermo) and low energy electron diffraction optics (BDL600, OCI). A $\text{TiO}_2(1\ 1\ 0)$ wafer of $7\ \text{mm} \times 1\ \text{mm} \times 0.3\ \text{mm}$ size (Shinko-sha) was cleaned by repetitions of Ar^+ sputtering and annealing at 1100 K in vacuum to obtain the (1×1) surface. A Si wafer placed behind the TiO_2 wafer was used as a resistive heater. The temperature was measured through the transparent TiO_2 wafer with an infrared pyrometer (TR630, Minolta) and was therefore overestimated. The obtained (1×1) surface was exposed to 900 L ($1\ \text{L} = 1 \times 10^{-6}$ Torr s) of pivalic acid ($(\text{CH}_3)_3\text{CCOOH}$) vapor at room temperature. The pivalic acid dissociates to form a pivalate ($(\text{CH}_3)_3\text{CCOO}^-$) and a proton on the (1×1) surface at room temperature [25]. The pivalate is anchored to two 5-fold-coordinated Ti atoms in the bridge form. At the saturation coverage, pivalates are packed with a (2×1) periodicity, thereby forming a monolayer. The left half of the (1×1) surface shown in Fig. 1(b) is covered by the pivalate monolayer. The pivalate monolayer is stable in the laboratory air and in the acetonitrile, and the chemically inert alkyl group exposed on the top surface prevents the TiO_2 surface from being polluted during the N3 adsorption process [4,6]. The pivalate-covered TiO_2 wafer was removed from the chamber and immersed in acetonitrile containing the N3 at room temperature. After immersion in the solution, the sample wafer was rinsed in pure acetonitrile for several seconds and reintroduced into the vacuum. N3 molecules physisorbed to the surface are expected to be removed in the rinsing. The STM images were acquired at room temperature in the constant current mode with a tungsten tip prepared by electrochemical etching of a tungsten wire. The X-ray photoelectron spectroscopy (XPS) analysis was performed in Ion Technology Center Co., Ltd. (Osaka, Japan) using a Mg $K\alpha$ source (1284.6 eV).

3. Results and discussion

Fig. 2(a) is an STM image of the TiO_2 surface exposed to pivalic acid vapor. Flat terraces separated by steps of 0.32 nm height were observed. The inset is a close-up of the terrace. The pivalates were observed as particles packed with a (2×1) periodicity. Fig. 2(b) shows the pivalate-covered surface after immersion in an acetonitrile solution of 3.4×10^{-3} M N3 for 1 min. Bright particles protruding by 0.6 nm appeared on the surface. The number density of the particles was $0.08\ \text{nm}^{-2}$. The surface composition ratios Ru/S and N/S were estimated to be 0.58 and 4.1, respectively, from the intensity of the Ru 3d $5/2$, N 1s, and S 2p XPS peaks. The ratios almost correspond to those obtained from the elemental composition of the N3 molecule (0.5 for Ru/S, 3 for N/S). Further immersion led to an increase in number density and size of the particles as shown in Fig. 2(c). Such particles were not observed on the surface immersed in pure acetonitrile and we therefore assigned the particles to N3 molecules which replaced the pivalates. The particles with the smallest diameter of ~ 1.2 nm were single N3 molecules, and the larger particles were clusters of the N3 molecules. The diameter of the single N3 molecules is comparable to that in images previously obtained with a tungsten tip, ~ 1.5 nm [6], whereas a larger diameter of ~ 2.0 nm was estimated in images obtained with a Si cantilever [5]. The tip attached to the cantilever was probably blunter than the tungsten tip as it inevitably touches the surface during noncontact atomic force microscope measurement.

The N3 molecule is probably trapped by a pivalate and replaces another nearby pivalate by analogy with the exchange reaction between the acetic acid (CH_3COOH) molecule and the formate (HCOO^-) [7]. Acetate (CH_3COO^-) and formate form monolayers on the (1×1) surface in a similar way to the pivalates. When acetic acid molecules impinge on a mixed monolayer of formate and acetate from the gas phase, the acetic acid molecule forms a hydrogen bond via the carboxyl group with the adsorbed acetate reconstructing from the bridge form to a monodentate form ($-\text{CO}-\text{O}-\text{Ti}$). The trapped acetic acid molecule eliminates the formate adjacent to the adsorbed acetate.

Fig. 2(d) is a close-up of the terrace of the surface shown in Fig. 2(b). The N3 molecules embedded in the pivalate monolayer were observed as bright particles and seemed to be located adjacent each other. Some of the pivalates were observed as less bright particles, and the dark areas indicated by arrows are the vacant sites where the pivalates were removed. The positions of the N3 molecules and the pivalates did not change during imaging, which indicates that the N3 molecules did not migrate. Any migration of the N3 molecule in the pivalate monolayer would require exchange between neighboring N3 molecule and pivalate anions. Such exchange reactions are known to be slow enough to be observed via time-lapse STM measurements from experiments on mixed monolayers of acetate and formate [26]. Migration of the adsorbed N3 molecules in the pivalate monolayer when they are in the acetonitrile solution is also unlikely, so the lateral distribution of the N3 molecules in the STM images should be identical to that in the solution.

To examine the lateral coordination of the N3 molecule, autocorrelation of the N3 molecules was calculated on the surfaces prepared by 1 min immersion. When applied to a microscope image, the two-dimensional autocorrelation function $F(i, j)$ provides the azimuth and distance of one N3 molecule relative to another [9,10]. $F(i, j)$ is given by

$$F(i, j) = \sum_{i,j} (f(x, y)f(x+i, y+j))^{1/2}$$

where $f(x, y)$ is image intensity at pixel (x, y) . We defined $f(x, y) = 1$ for the pixel at the center of each N3 molecule and $f(x, y) = 0$ for

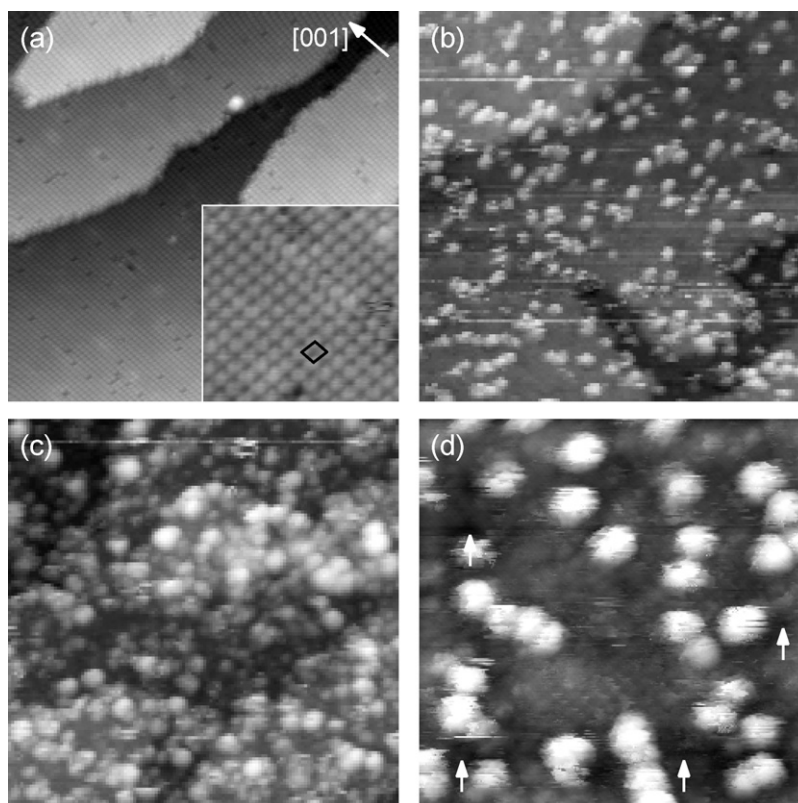


Fig. 2. (a)–(d) Constant current images of the pivalate-covered TiO_2 surfaces. (a) Before immersion in the N3 solution ($50 \text{ nm} \times 50 \text{ nm}$). The inset shows a close-up of the terrace ($7.5 \text{ nm} \times 7.5 \text{ nm}$). The square shows the (2×1) unit cell. (b) After immersion in $3.4 \times 10^{-3} \text{ M}$ N3 solution for 1 min ($50 \text{ nm} \times 50 \text{ nm}$). (c) After immersion in $3.4 \times 10^{-3} \text{ M}$ N3 solution for 10 min ($50 \text{ nm} \times 50 \text{ nm}$). (d) A close-up of the surface shown in (b) ($20 \text{ nm} \times 20 \text{ nm}$). Sample bias voltage (V_s) = +1.0 V, tunneling current (I_t) = 1.0 nA.

other pixels. Then $F(0, 0)$, the sum of the self-image of each N3 molecule, is equal to the number of N3 molecules. Here we consider the function $F(i, j)/F(0, 0)$ which corresponds to the number ratio of the N3 molecules finding another molecule at (i, j) .

$F(i, j)/F(0, 0)$ was calculated for 1035 N3 molecules in 27 images of $30 \text{ nm} \times 30 \text{ nm}$ width. To obtain the $F(i, j)/F(0, 0)$ map of $8.0 \text{ nm} \times 8.0 \text{ nm}$ width, the N3 molecules in the central $26 \text{ nm} \times 26 \text{ nm}$ areas of the images were analyzed to examine lateral coordination with other N3 molecules in all lateral azimuths. The N3 molecules adsorbed on the terraces were analyzed but those within belts of 1 nm width along the steps were ignored. This is because our previous STM study revealed that the N3 molecules preferentially adsorb along the steps [6]. As the steps of the (110) surface are elongated preferentially along the $\langle 001 \rangle$ and $\langle 1\bar{1}1 \rangle$ directions [27], an $F(i, j)/F(0, 0)$ map which considered all the N3 molecules would show not the lateral distribution of the N3 molecules but the line density of the step edges.

The obtained $F(i, j)/F(0, 0)$ map is shown in Fig. 3(a). A bright ring was observed around the center $(0, 0)$. The cross sections along the dotted lines through the center were shown in Fig. 3(b). The distance r from the center was estimated to be 1.2 nm for the inner periphery of the ring and is comparable with the lateral size of single N3 molecules in the STM images. Therefore, the bright ring indicates that the number ratio of N3 molecules with neighboring N3 molecules, which are defined here as aggregated, was larger than that of the N3 molecules which found N3 molecules at other places. The fraction of N3 molecules located with a separation of 1.2–1.6 nm was estimated to be 70% from the STM images. The homogenous brightness of the ring means that the aggregated N3 molecules were present in all azimuthal directions.

The histogram of Fig. 3(c) shows the radial distribution of $F(i, j)/F(0, 0)$ as a function of the r . The $F(i, j)$ with the (i, j) satis-

fying $(i^2 + j^2)^{1/2} = r$ was designated as $F(r)$. The $F(r)/F(0)$ values were summed up and then normalized by the total area of the pixels, $S(r)$. The histogram showed a peak in the range of 1.4–1.6 nm, and the peak reached 190% of the average value in the range from 1.8 to 5.0 nm. The high probability of finding neighboring N3 molecules was well contrasted by the radial distribution of randomly arranged spots. The histogram of Fig. 3(d) was obtained from 835 spots randomly arranged with the same number density as that of the N3 molecules. The $\{ \sum F(r)/F(0) \} / S(r)$ values are constant within a 10% deviation from the entire average value.

One explanation for the N3 aggregation is that the preadsorbed N3 molecules trapped other N3 molecules in the acetonitrile solution. The N3 molecule embedded in the pivalate monolayer has two free carboxyl groups [6] which are likely to trap the N3 molecule in the acetonitrile solution via hydrogen bonds between the carboxyl groups. The trapping of the N3 molecules enhances the local concentration of the N3 molecule around the adsorbed N3 molecule. The trapped N3 molecule would be released and replace the neighboring pivalate, which results in the uniform distribution in all azimuths around the preadsorbed N3 molecules. By considering the directivity of the hydrogen bonds, it is less likely that the trapped N3 molecule is bound to the pivalate to form N3-N3-pivalate species, even if structural relaxation of the adsorbed N3 molecule occurs. The contribution of the carboxyl groups towards aggregation was also indicated in our previous study of the black dye molecule [4]. The STM observation revealed that the aggregation of the black dye molecules was suppressed by adding deoxycholic acid in the black dye solution. The deoxycholic acid probably fills the carboxyl groups of the black dye molecules by forming a hydrogen bond.

Another possible cause for the aggregation is intact adsorption of N3 molecules associated in acetonitrile. It is likely that N3 molecules are associated by hydrogen bonds between the car-

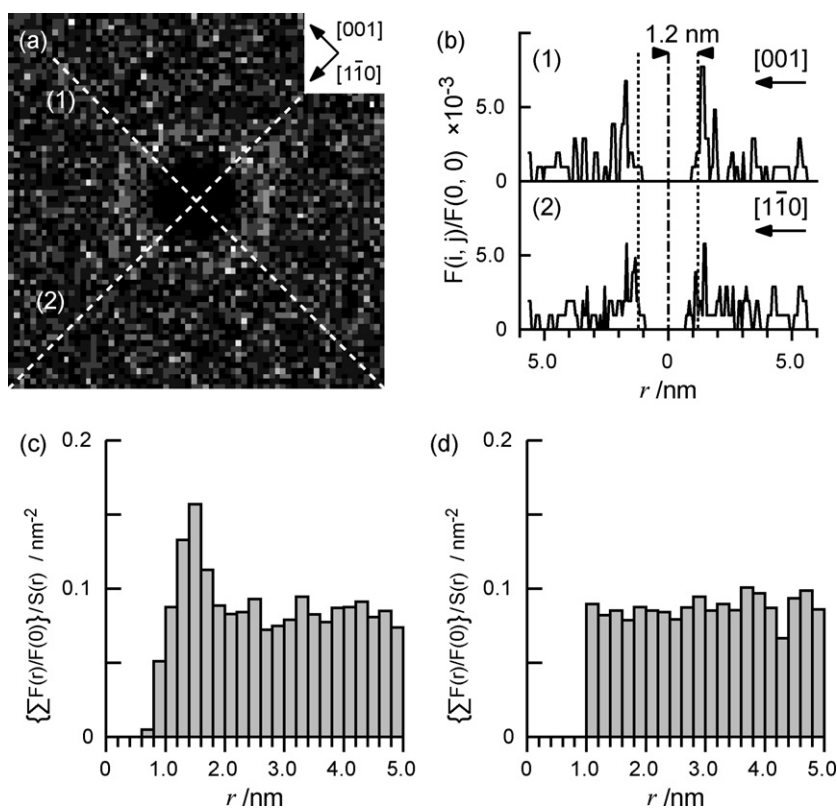


Fig. 3. (a) The map of the normalized autocorrelation function for the N3 molecules on the TiO₂(1 1 0) surface (8 nm × 8 nm). The central spot $F(0, 0)$ was removed. (b) Cross sections along the dotted lines in the map (a). (c) The distribution of the $\{\Sigma F(r)/F(0)\}/S(r)$ values obtained for the N3 molecules. (d) The distribution of the $\{\Sigma F(r)/F(0)\}/S(r)$ values obtained for the spots randomly distributed.

boxyl groups. The probability of the association depends on the N3 concentration. Fig. 4 shows an STM image of the pivalate-covered TiO₂ surface immersed in 2.0×10^{-5} M N3 solution. On the surface immersed for 30 sec, single N3 molecules (solid arrowheads) and aggregates of N3 (open arrowheads) were observed as shown in Fig. 4(a). The number ratio of the aggregates to all the particles was 25%, although the obtained number ratio is a lower limit because individual N3 molecules in some aggregates were not resolved. When the immersion time was extended to 5 min, the number ratio of the aggregates increased to 70% as shown in Fig. 4(b). The dependence of the fraction of N3 molecules which aggregate on the immersion time suggests a minor contribution of the intact adsorption. The observed positive dependence is interpreted as consecutive N3 adsorption from the solution.

We consider adsorption sites for two N3 molecules with a separation of 1.2–1.6 nm. Fig. 5(a) shows two possible configurations of the N3 molecule adsorbed on the (1 × 1) surface [6]. A free N3 molecule is superimposed above the TiO₂ surface, and the 5-fold-coordinated Ti atoms bound to the carboxyl groups are marked by the dotted-line circles in the models of the surface. In configuration (i), two carboxyl groups of the same bipyridine ring are anchored in a bridge form to the Ti atoms (Ti–O–C–O–Ti). The bridge sites of the Ti atoms are aligned in the $(\bar{1} \ 1 \ \bar{1})$ direction. The maximum lateral width defined by atom-atom distance is the width of the free bipyridine ligand, 1.0 nm. When the N3 molecule is adsorbed via two carboxyl groups from different bipyridine rings as shown in (ii), the anchored two carboxyl groups lie along the $(\bar{1} \ 1 \ \bar{3})$ direction. The lateral distance between the free carboxyl group and the anchored

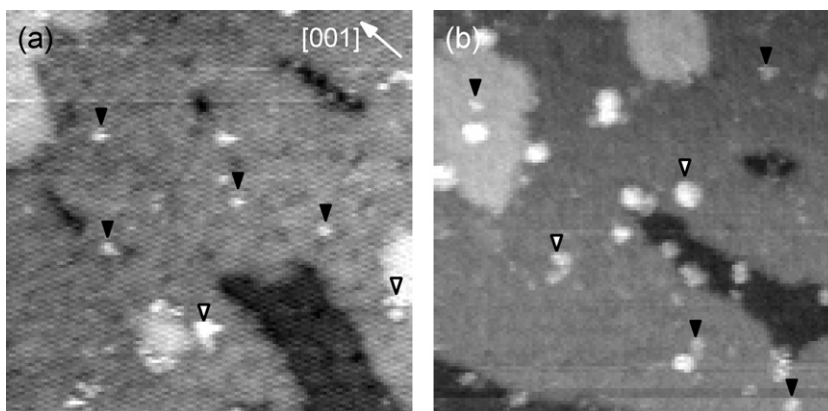


Fig. 4. Constant current image of the pivalate-covered TiO₂ surface immersed into 2.0×10^{-5} M N3 solution for (a) 30 s and (b) 5 min (50 nm × 50 nm). Some isolated N3 molecules and N3 aggregates are marked by solid and open arrowheads, respectively. $V_s = +1.0$ V, $I_t = 0.1$ nA.

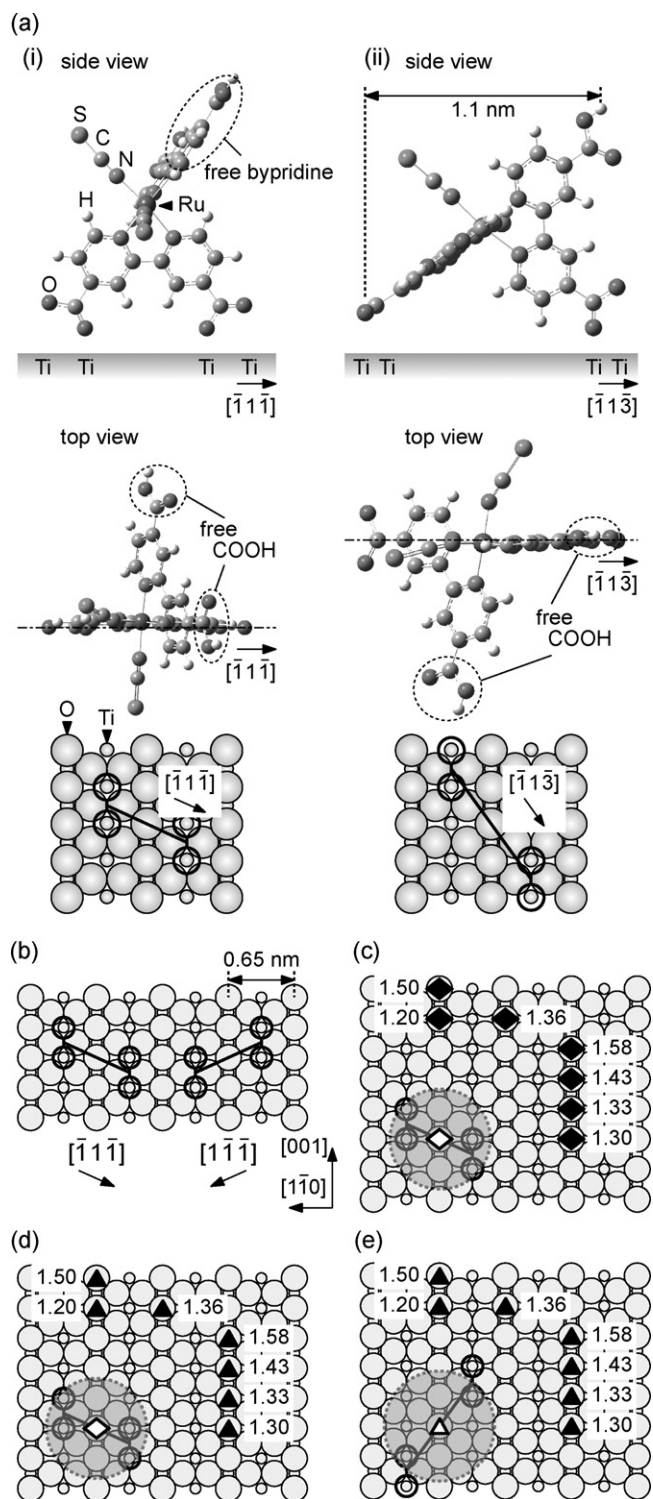


Fig. 5. (a) Possible adsorption configurations for the N3 molecule on the $\text{TiO}_2(110)$ - (1×1) surface [6]. Hydrogen atoms of the anchored carboxyl groups are removed, and twist of OCO planes relative to pyridine ring planes is not included. In the ball model of the (1×1) surface, the Ti atoms bound to the carboxyl groups are marked by circles. (b) The two possible arrangements of the N3 molecule in configuration (i). The surface Ti atoms bound to the carboxyl groups are marked by circles. (c)–(e) Adsorption sites for two N3 molecules with a separation of 1.2–1.6 nm. The middle of the anchored carboxyl groups are marked by diamonds (configuration (i)) or triangles (configuration (ii)). The distances between the open and solid symbols are annotated in nanometer scale. The dotted-line circles show the lateral width of the N3 molecules estimated from the atom-atom distance. (c) Both N3 molecules have configuration (i). (d) One N3 molecule has configuration (i) and the other, configuration (ii). (e) Both N3 molecules have configuration (ii).

carboxyl group opposite, 1.1 nm, corresponds to the lateral width.

Fig. 5(b) shows the two bridge sites where the carboxyl groups of the N3 molecule in the configuration (i) are anchored. The two arrangements of the bridge sites of the Ti atoms along the $[\bar{1}1\bar{1}]$ and $[1\bar{1}\bar{1}]$ directions are symmetric with respect to the $[001]$ and $[1\bar{1}0]$ directions. Suppose that the N3 molecule has a rigid structure and the two carboxyl groups anchoring to the surface are switched between the two bridge sites. The structure of the free bipyridine ligand is symmetric with respect to the center of the two bridge sites. Hence, the directions of the free carboxyl groups are symmetric with respect to the $[001]$ and $[1\bar{1}0]$ directions. Such symmetry of the free carboxyl groups holds true for the N3 molecule adsorbed in the configuration (ii). Therefore, just one quadrant of the coordinate from the N3 molecule was considered.

The possible adsorption sites are shown in Fig. 5(c)–(e). Diamonds and triangles represent the N3 molecules with configurations (i) and (ii), respectively. The symbols are located at the middle between the two carboxyl groups anchored to the surface. N3 molecule indicated by solid symbols are placed around another N3 molecule indicated by an open symbol. The dotted-line circles show the lateral width of the N3 molecules estimated from the atom-atom distance. Fig. 5(c) shows the adsorption sites for two N3 molecules with configuration (i). The possible adsorption sites are present in all lateral azimuths. When an N3 molecule with configuration (ii) is arranged around a preadsorbed N3 molecule with configurations (i) or (ii), possible adsorption sites are also present in all azimuths as shown in Fig. 5(d) and (e), respectively. Thus adsorption sites with separations of 1.2–1.6 nm are provided for the trapped N3 molecule in all direction around the preadsorbed N3 molecule.

4. Conclusion

Aggregation of N3 molecules was revealed on a pivalate-covered rutile $\text{TiO}_2(110)$ by applying the autocorrelation analysis to molecularly resolved STM images. Trapping of N3 molecules in the solution by a preadsorbed N3 molecule was proposed as the driving force for the aggregation. The STM analysis employing model surfaces is a possible approach to reveal the aggregation process of the dye molecules, which could lead to the control of the distribution of the dye molecules.

Acknowledgements

The present work was supported by the New Energy and Industrial Technology Development Organization (NEDO) in association with the Ministry of Economy, Trade and Industry, and by a Grant-in-Aid for Scientific Research (KAKENHI) on Priority Areas (477) 'Molecular Science for Supra Functional Systems' from the Ministry of Education, Culture, Sports, Science and Technology (MEXT), Japan.

References

- [1] M. Grätzel, *Chem. Lett.* 34 (2005) 8–13.
- [2] S. Yanagida, *C. R. Chimie* 9 (2006) 597–604.
- [3] Y. Chiba, A. Islam, Y. Watanabe, R. Komiya, N. Koide, L. Han, *Jpn. J. Appl. Phys.* 45 (2006) L638–L640.
- [4] M. Ikeda, N. Koide, L. Han, A. Sasahara, H. Onishi, *Langmuir* 24 (2008) 8056–8060.
- [5] M. Ikeda, N. Koide, L. Han, A. Sasahara, H. Onishi, *J. Phys. Chem. C* 112 (2008) 6961–6967.
- [6] A. Sasahara, C.L. Pang, H. Onishi, *J. Phys. Chem. B* 110 (2006) 4751–4755.
- [7] H. Uetsuka, T. Ishibashi, A. Sasahara, H. Onishi, *J. Phys. Chem. B* 107 (2003) 9939–9942.
- [8] J.V. Barth, *Surf. Sci. Rep.* 40 (2000) 75–149.
- [9] H. Onishi, K. Fukui, Y. Iwasawa, *Jpn. J. Appl. Phys.* 38 (1999) 3830–3832.
- [10] U. Diebold, W. Hebenstreit, *Phys. Rev. Lett.* 81 (1998) 405–408.

- [11] Z.-S. Wang, Y. Cui, Y. Dan-oh, C. Kasada, A. Shinpo, K. Hara, J. Phys. Chem. C 111 (2007) 7224–7230.
- [12] Z.-S. Wang, K. Hara, Y. Dan-oh, C. Kasada, A. Shinpo, S. Suga, H. Arakawa, H. Sugihara, J. Phys. Chem. B 109 (2005) 3907–3914.
- [13] B. Wenger, M. Grätzel, J. Moser, J. Am. Chem. Soc. 127 (2005) 12150–12151.
- [14] K. Hara, Y. Dan-oh, C. Kasada, Y. Ohga, A. Shinpo, S. Suga, K. Sayama, H. Arakawa, Langmuir 20 (2004) 4205–4210.
- [15] K. Hara, H. Sugihara, Y. Tachibana, A. Islam, M. Yanagida, K. Sayama, H. Arakawa, Langmuir 17 (2001) 5992–5999.
- [16] K. Keis, J. Lindgren, S. Lindquist, A. Hagfeldt, Langmuir 16 (2000) 4688–4694.
- [17] A. Fillinger, B.A. Parkinson, J. Electrochem. Soc. 146 (1999) 4559–4564.
- [18] M.K. Nazeeruddin, A. Kay, I. Rodicio, R. Humphry-Baker, E. Müller, P. Liska, N. Vlachopoulos, M. Grätzel, J. Am. Chem. Soc. 115 (1993) 6382–6390.
- [19] S. Fantacci, F.D. Angelis, A. Selloni, J. Am. Chem. Soc. 125 (2003) 4381–4387.
- [20] N.W. Duffy, K.D. Dobson, K.C. Gordon, B.H. Robinson, A.J. McQuillan, Chem. Phys. Lett. 266 (1997) 451–455.
- [21] A. Hugot-Le Goff, P. Falaras, J. Electrochem. Soc. 142 (1995) L38–L41.
- [22] P. Falaras, M. Grätzel, A. Hugot-Le Goff, E. Vrachnou, J. Electrochem. Soc. 140 (1993) L92–L94.
- [23] K.S. Finnie, J.R. Bartlett, J.L. Woolfrey, Langmuir 14 (1988) 2744–2749.
- [24] U. Diebold, Surf. Sci. Rep. 48 (2003) 53–229.
- [25] A. Sasahara, H. Uetsuka, T. Ishibashi, H. Onishi, J. Phys. Chem. B 107 (2003) 13925–13928.
- [26] H. Uetsuka, A. Sasahara, A. Yamakata, H. Onishi, J. Phys. Chem. B 106 (2002) 11549–11552.
- [27] U. Diebold, J. Lehman, T. Mahmoud, M. Kuhn, G. Leonardelli, W. Hebenstreit, M. Schmid, P. Varga, Surf. Sci. 411 (1998) 137–153.